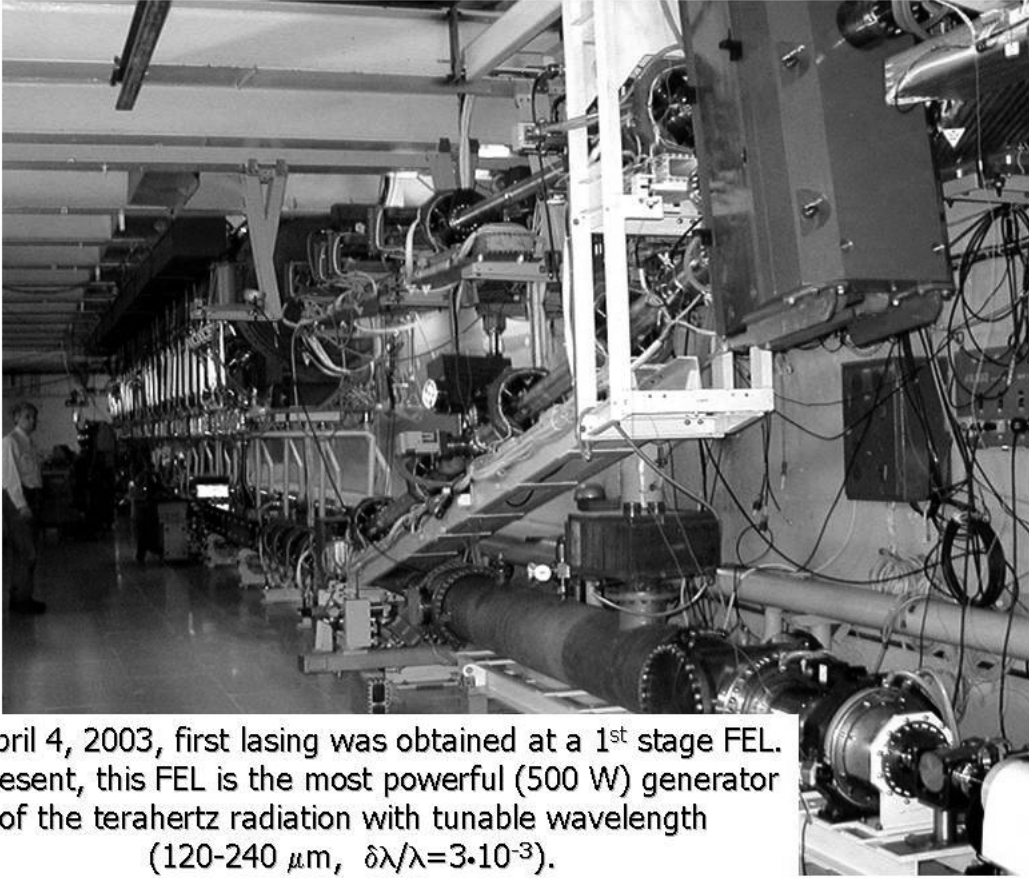
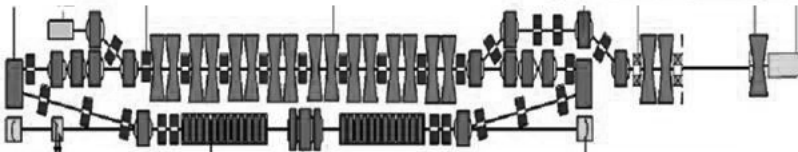
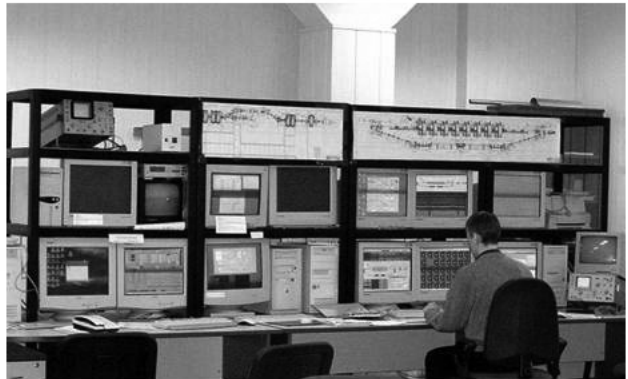
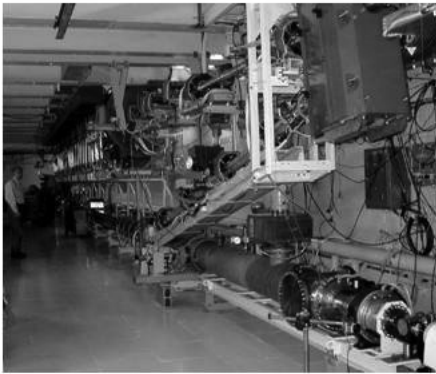


Novosibirsk FEL (NovoFEL) as prototype of MARS



On April 4, 2003, first lasing was obtained at a 1st stage FEL. At present, this FEL is the most powerful (500 W) generator of the terahertz radiation with tunable wavelength (120-240 μm , $\delta\lambda/\lambda=3\cdot 10^{-3}$).

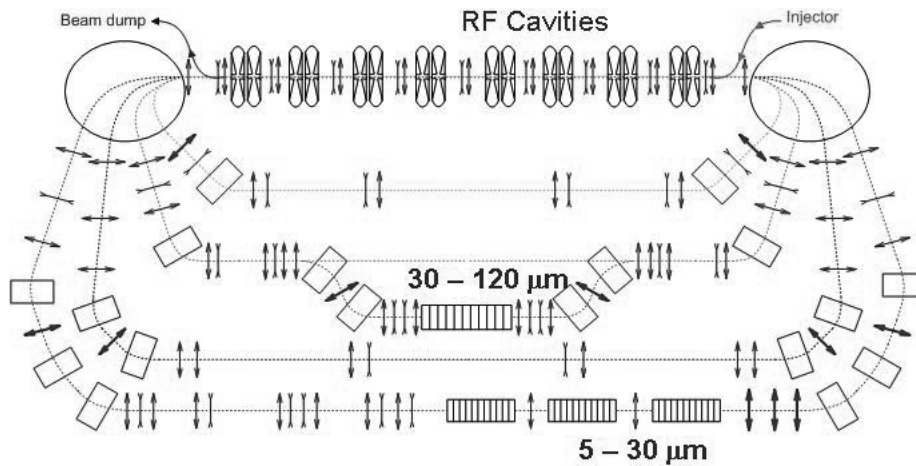
49



The scheme and views of the 1st stage Novosibirsk accelerator-recuperator and FEL

50

The 2nd and 3rd stages of Novosibirsk FEL placed in the horizontal plane (prototype of MARS)



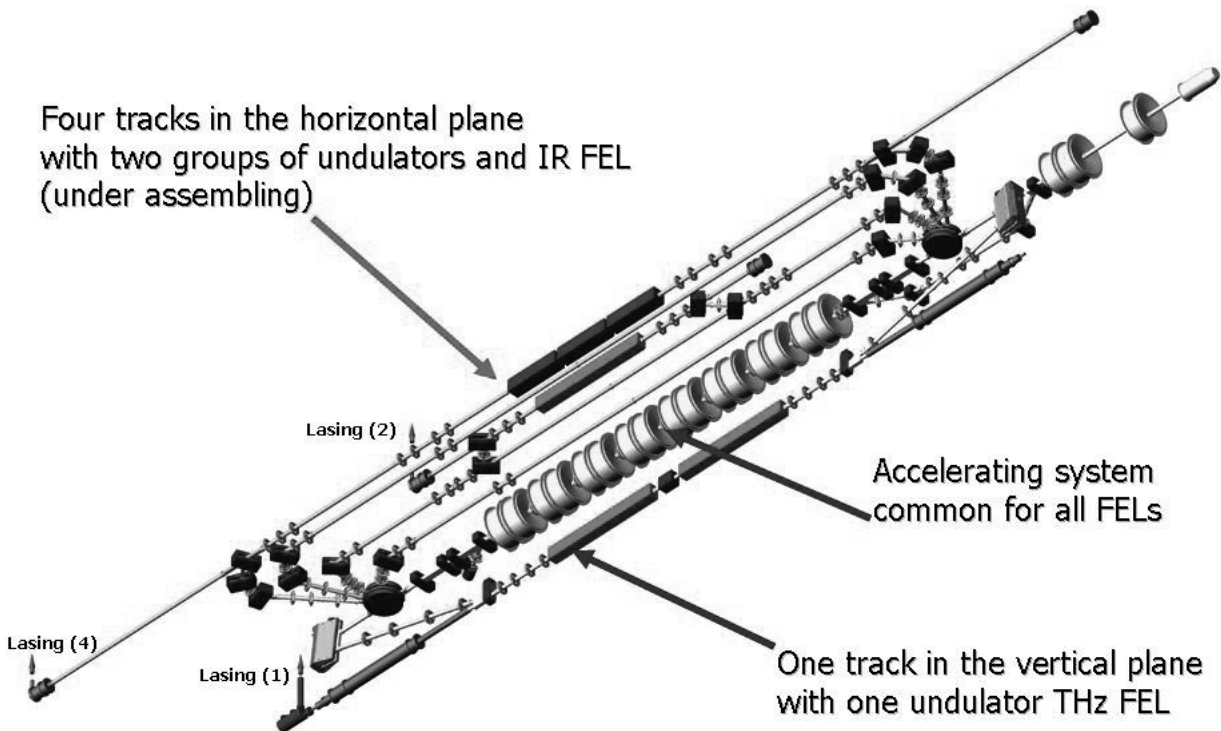
Radiation wavelength	5 – 240 μm
Average power	Up to 10 kW
E-beam energy	up to 40 MeV
Maximum repetition rate	90 MHz
Maximum mean current	150 mA

Taking into account the 120 – 240 μm 1st stage NovoFEL placed in the vertical plane

51

Full scale Novosibirsk FEL

Four tracks in the horizontal plane with two groups of undulators and IR FEL (under assembling)



52

On February 2, 2009, first lasing ($\lambda=50 \mu\text{m}$) was achieved on the 2nd stage FEL (the 2-turn AR)

Second turn

First turn

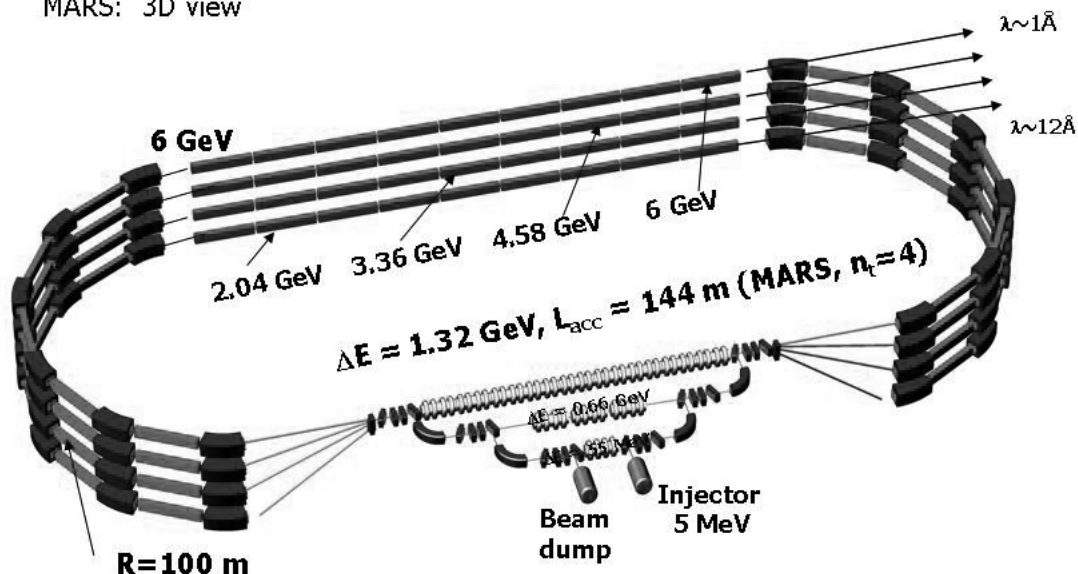
Undulator of the 2nd stage
NovoFEL

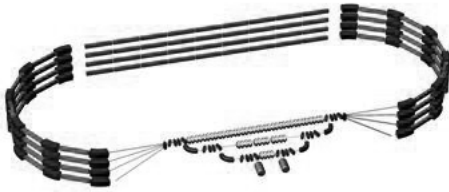
53

MARS – diffraction limited coherent X-ray source for national or international SR centers

Conceptual scheme of MARS ($E_{\text{max}} = 6 \text{ GeV}$)

MARS: 3D view



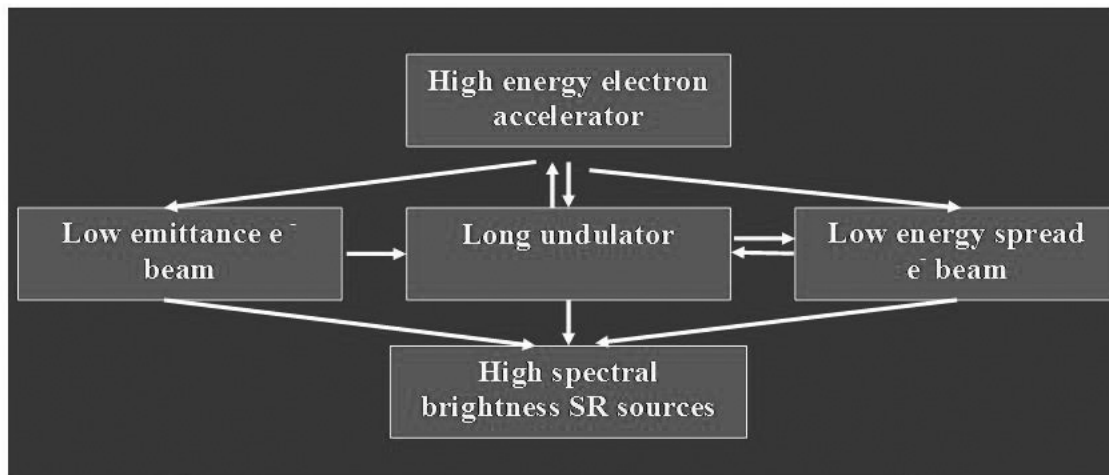


- In MARS, the electrons obtained in the injector with an energy of ~ 5 MeV are then accelerated in an additional two-cascade injector, after which they pass through the main accelerating high-frequency structure four times, thus increasing their energy up to 6 GeV.
- After acceleration, the electrons again travel in the same direction through the same high-frequency structures but in a deceleration phase, decrease their energy to 5 MeV, and then land in the dump. In the MARS, electrons undergoing acceleration and deceleration travel simultaneously along four tracks.

55

- Users of synchrotron radiation will perceive radiation from the MARS undulators like radiation from a storage ring, with the only difference that each time new ('fresh') electrons are used with a small emittance $\varepsilon_{\min} \sim 10^{-11}$ m·rad and energy spread $\sigma_E/E \sim 10^{-4}$.
- For the MARS project, four undulators 150 – 200 m long ($N \sim 10^4$) are placed in the four tracks as well as several dozen undulators 5 – 20 m long ($N = 10^2 - 10^3$) in the arcs.

56



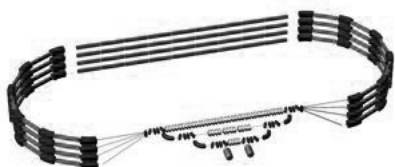
1980	$\epsilon \sim 300 \text{ nmrad}$	$N_u \sim 10$	$\sigma_E/E \sim 10^{-3}$
1990	$\epsilon \sim 30 \text{ nmrad}$	$N_u \sim 10^2$	$\sigma_E/E \sim 10^{-3}$
2000	$\epsilon \sim 3 \text{ nmrad}$	$N_u \sim 10^3$	$\sigma_E/E \sim 10^{-3}$
2010	$\epsilon \sim 1 \text{ nmrad}$	$N_u \sim 10^3$	$\sigma_E/E \sim 10^{-3}$
2020	$\epsilon \sim 0.01 \text{ nmrad}$	$N_u \sim 10^4$	$\sigma_E/E \sim 10^{-4}$

Storage rings

MARS

57

Comparison of the parameters of the SR sources
MARS ($I_e=2.5 \text{ mA}$) and Spring-8 ($I_e=100\text{mA}$)



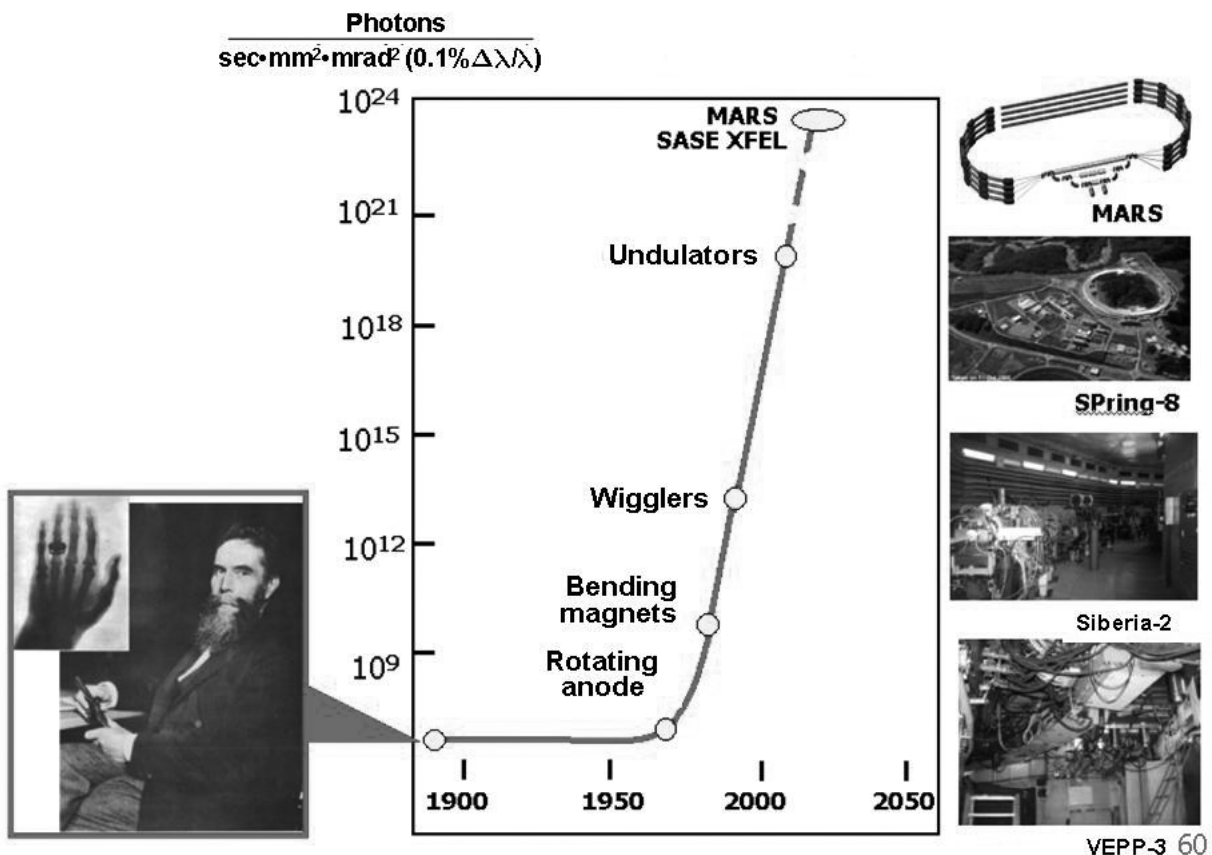
		Number of beamlines	$B, \text{ ph}\cdot\text{sec}^{-1}\cdot\text{mm}^{-2}\cdot\text{mrad}^{-2}$ ($\delta\lambda/\lambda=10^{-3}$)	$F, \text{ ph}/\text{sec}$ ($\delta\lambda/\lambda=10^{-3}$)
MARS	Undulator $N_u \sim 10^2$	32	10^{22}	$4.6 \cdot 10^{13}$
	Undulator $N_u \sim 10^3$	12	10^{23}	$4.6 \cdot 10^{14}$
	Undulator $N_u \sim 10^4$	4	10^{24}	$4.6 \cdot 10^{15}$
Spring-8	Bending magnet	23	10^{16}	10^{13}
	Undulator $N_u=130$	34	$3 \cdot 10^{20}$	$2 \cdot 10^{15}$
	Undulator $N_u=780$	4	10^{21}	$1.2 \cdot 10^{16}$

Comparison of various types of the coherent X-ray sources:

	ESRF storage ring	LCLS linac	MARS
Wavelength, nm	.1	.15	.1
Electron energy, GeV	6	14	5.4
Average current, A	.2	3×10^{-8}	10^{-3}
Peak current, A		3.4×10^3	1
Relative energy spread		2×10^{-4}	1×10^{-5}
Emittance, nm ϵ_x	4	5×10^{-2}	3×10^{-3}
ϵ_z	2.5×10^{-2}		
Undulator period, cm	4.2	3	1.5
Undulator length, m	5	120	150
Coherent flux, photon/s	6×10^{12}	2×10^{14}	7×10^{13}
Bandwidth	10^{-2}	10^{-3}	10^{-4}
Average brightness, ph/s/mm ² /mrad ² /0.1 %BW	10^{20}	4×10^{22}	3×10^{23}
Peak brightness, —//—		1×10^{33}	3×10^{26}
Transverse size of source (standard deviation), μm	σ_x 350 σ_y 8	15	10
Radiation transverse divergence (standard deviation), μrad	σ_x 13 σ_y 3	1	1

59

Steep rise in average brightness

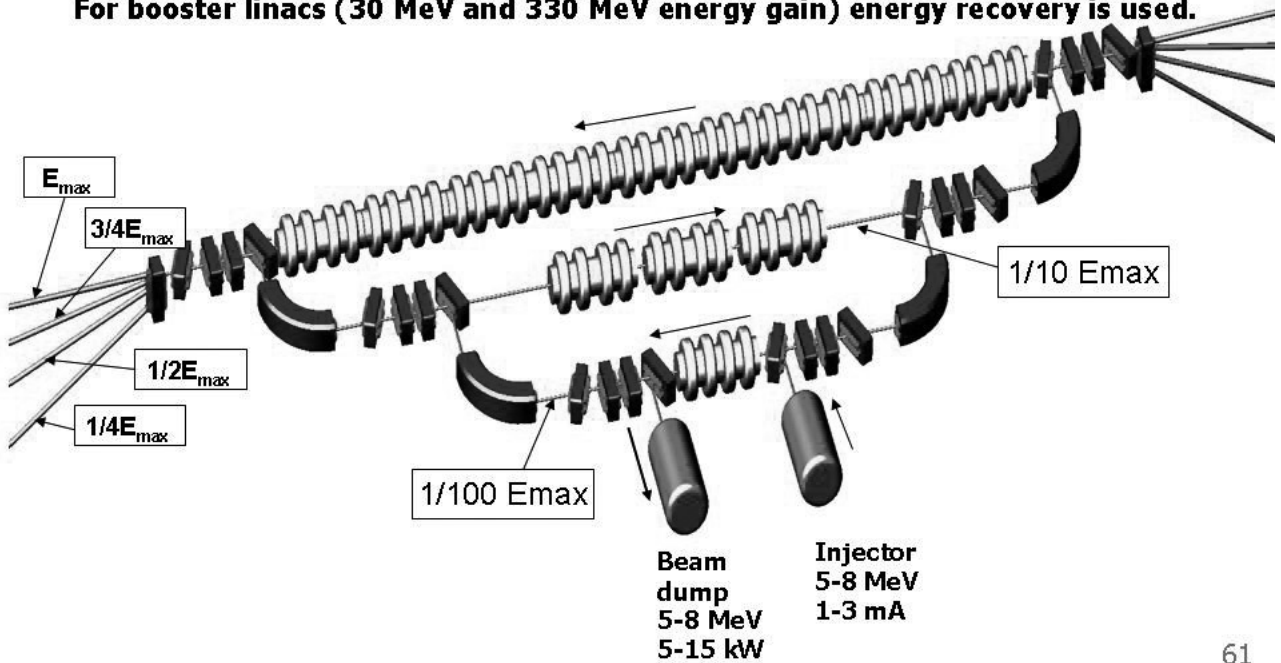


VEPP-3 60

Some technical solutions
for realization of the 4th generation SR sources
on the base of accelerators-recuperators

Cascade injection

**First linac has 5-8 MeV energy and does not use energy recovery.
For booster linacs (30 MeV and 330 MeV energy gain) energy recovery is used.**



61

Cascade scheme of injection provides effective and economical solution to the following problems:

- Decrease in radiation hazard and limitation of induced radioactivity;
- Reduction in the cost of construction and RF power system for the injector;
- and simplifies the problem of focusing particles of different energies traveling simultaneously in the accelerating structure, because the cascade scheme enables injection of electrons into all accelerating structures with energies of no less than $E_{max}/10$ (E_{max} is the maximum energy of electrons traveling in the accelerating structure).

62

Electron gun

- In recirculating accelerators—recuperators (single or multi-pass), the electron gun must produce low emittance of electron beam ε_n . Then, owing to adiabatic damping during acceleration up to high energies ($E > 5$ GeV, $\gamma > 10^4$), it is possible to obtain emittance

$$\varepsilon_{x,z} = \frac{\varepsilon_n}{\gamma}$$

- For diffraction-limited X-ray sources, emittance of electron beam at final energy must be $\varepsilon_{x,z} < \frac{\lambda}{4\pi}$ for $\lambda = 0.1$ nm,
 $\varepsilon_{x,z} < 10^{-11}$ m·rad.

63

Photoemission offers several advantages over thermal emission:

- higher current density;
- bunched beams are generated through a laser with ~ 10 ps bunches of an appropriate time structure, readily available from photocathodes: no need for chopping as in case of thermal emission;
- a colder beam (lower thermal emittance) is possible.

64

- minimum possible normalized emittance, determined by the initial thermal energy spread, is fundamental and uncorrectable

$$\varepsilon_n = \frac{r_c}{2} \left(\sqrt{\frac{E_{thermal}}{mc^2}} \right)^{1/2}$$

$$\varepsilon_n = (1.5 \div 4.5) 10^{-4} r \quad E_{thermal} = (35 \div 300) meV$$

65

- distortion of the phase space and emittance growth due to RF time-dependent effects and space charge-induced effects could be corrected (long RF wave length, using photocathodes, small peak current, high accelerating gradient ...)
- the normalized emittance $\varepsilon_n < 10^{-7}$ m·rad has been obtained for bunches of electrons with the charge $Q = 7.7 \cdot 10^{-12}$ Coul and duration $\tau_{pulse} = 14$ ps

(ERL-2005).

66

Main requirements to the photoinjector photocathode of accelerator – recuperator:

- CW operation (up to 1.3 GHz);
- operable in high field (> 5 MV/m);
- high average current – (up to 10 mA);
- high quantum efficiency (5 – 10) %;
- long operational lifetime ($10^3 \div 10^4$ hours);
- small thermal emittance ($\varepsilon_n < 10^{-7}$ m-rad);
- small cathode dark current ($I < 10$ pA at gradient more than 5 MV/m);
- prompt response time (~ 100 fs);
- short recovery time.

67

Four families of high quantum efficiency photocathodes:

1. alkali antimonide (K_2GsSb) cathodes;
2. alkali telluride ($KCsTe$) cathodes;
3. negative electron affinity (NEA) semiconductor ($CsGaAs$) cathodes. NEA semiconductor cathodes have an additional advantage – very small thermal emittance and better quantum efficiency;
4. diamond amplified photocathodes.

68